Title: Joint analysis of extracellular spike waveforms and neuronal network bursts

Author: Fikret Emre Kapucu Meeri E.-L. Mäkinen Jarno M.A. Tanskanen Laura Ylä-Outinen Susanna Narkilahti Jari A.K. Hyttinen

PII: S0165-0270(15)00424-0
DOI: http://dx.doi.org/doi:10.1016/j.jneumeth.2015.11.022
Reference: NSM 7398

To appear in: *Journal of Neuroscience Methods*

Received date: 2-6-2015
Revised date: 23-11-2015
Accepted date: 24-11-2015

Please cite this article as: Kapucu FE, Mäkinen ME-L, Tanskanen JMA, Ylä-Outinen L, Narkilahti S, Hyttinen JAK, Joint analysis of extracellular spike waveforms and neuronal network bursts, *Journal of Neuroscience Methods* (2015), http://dx.doi.org/10.1016/j.jneumeth.2015.11.022

Highlights

- Spike and burst statistics give limited information on changes in networks.
- Here, spike sorting combined with burst detection.
- Spike waveform type participation in bursts revealed.
- Spike type compositions of bursts change under network modifications.
- New kind of information obtained on the changes in bursting networks.

Joint analysis of extracellular spike waveforms and neuronal network bursts

Fikret Emre Kapucu[a], Meeri E.-L. Mäkinen[b], Jarno M. A. Tanskanen[a], Laura Ylä-Outinen[b], Susanna Narkilahti[b], Jari A. K. Hyttinen[a]

[a] Tampere University of Technology, Department of Electronics and Communications Engineering, Computational Biophysics and Imaging Group, BioMediTech, Tampere, Finland, Biokatu 6, FI-33520 Tampere, Finland

E-mail: fikret.kapucu@tut.fi, tanskanen@ieee.org, jari.hyttinen@tut.fi

[b] University of Tampere, NeuroGroup, BioMediTech, Tampere, Finland, Biokatu 12, FI-33014 University of Tampere, Finland

E-mail: meeri.makinen@uta.fi, laura.yla-outinen@uta.fi, susanna.narkilahti@uta.fi

Corresponding Author:

F. Emre Kapucu

Department of Electronics and Communications Engineering, Tampere University of Technology

Postal Address: Finn-Medi 1 L 4 (room 4-212), Biokatu 6, FI-33520 Tampere, Finland

E-mail: fikret.kapucu@tut.fi

Tel: +358 40 849 0023

Fax: +358 3 364 1385 (departmental fax not at the corresponding author's location, usage discouraged)

Abstract

Background: Neuronal networks are routinely assessed based on extracellular electrophysiological microelectrode array (MEA) measurements by spike sorting, and spike and burst statistics. We propose to jointly analyze sorted spikes and detected bursts, and hypothesize that the obtained spike type compositions of the bursts can provide new information on the functional networks.

New Method: Spikes are detected and sorted to obtain spike types and bursts are detected. In the proposed joint analysis, each burst spike is associated with a spike type, and the spike type compositions of the bursts are assessed.

Results: The proposed method was tested with simulations and MEA measurements of *in vitro* human stem cell derived neuronal networks under different pharmacological treatments. The results show that the treatments altered the spike type compositions of the bursts. For example, 6-cyano-7-nitroquinoxaline-2,3-dione almost completely abolished two types of spikes which had composed the bursts in the baseline, while bursts of spikes of two other types appeared more frequently. This phenomenon was not observable by spike sorting or burst analysis alone, but was revealed by the proposed joint analysis.

Comparison with Existing Methods: The existing methods do not provide the information obtainable with the proposed method: for the first time, the spike type compositions of bursts are analyzed.

Conclusions: We showed that the proposed method provides useful and novel information, including the possible changes in the spike type compositions of the bursts due to external factors. Our method can be employed on any data exhibiting sortable action potential waveforms and detectable bursts.

Keywords

Neuronal network; Microelectrode array; Burst detection; Spike waveform; Spike sorting; Electrophysiological signal analysis

Highlights

- Spike and burst statistics give limited information on changes in networks.
- Here, spike sorting combined with burst detection.
- Spike waveform type participation in bursts revealed.
- Spike type compositions of bursts change under network modifications.
- New kind of information obtained on the changes in bursting networks.

1. Introduction

Regardless of decades of research, neuronal networks, and their development and functioning, are still not fully understood. The analysis of electrophysiological data is one of the methodologies for advancing our knowledge. Developing new methods to derive more information from the available measurement data is highly desirable. Here, we propose a new joint spike and burst analysis method for analyzing extracellular network electrophysiology data. We illustrate the method with simulated signals, and as the test bench we use human stem cell derived neuronal networks cultured on microelectrode arrays (MEAs). Such networks have been shown to develop spontaneous electrical activity and show histiotypic behavior (Bużańska et al., 2005, 2006; Heikkilä et al., 2009).

MEAs are commonly employed in the assessment of the electrical activity of neuronal networks both *in vitro* and *in vivo*. MEA recordings carry information on the electrical activity in tissues and cell cultures at network and cell levels (Gross et al., 1977; Thomas et al., 1972; Pine, 1980; Egert et al., 1998), e.g., from neurons in the vicinity of the MEA electrodes. Physically, MEAs record extracellular field potentials as voltage signals, which can exhibit contributions from both action potentials and lower frequency neuronal activity, in addition to noise. Here, we consider that an action potential is synonymous with a voltage spike over any area of neuronal cell membrane recorded via a MEA electrode. In the recordings, spikes may occur as individual spikes, or as trains or bursts manifesting network activity. (Kandel and Spencer, 1961; Connors et al., 1982; Gray and McCormick, 1996).

To use neuronal networks on MEAs as biosensors was proposed by Gross and Rhoades (1995), who described the effects of several pharmacological agents on bursting, and also mentioned the possibility to measure average spike waveforms. Several studies have suggested various spike and burst related metrics to quantify neuronal network behavior (Bal-Price et al., 2008; Johnstone et al., 2010; Defranchi et al., 2011; Hogberg et al., 2011; Novellino et al., 2011; Alloisio et al., 2015). In previous studies, parameters such as spike count, the number of bursts, mean spike rate, mean burst rate, the number of spikes in bursts, burst duration, interburst interval, and the percentage of spikes in bursts have been commonly used (Johnstone et al., 2010; Novellino et al., 2011; Uchida et al., 2012). Furthermore, patterns and spatial distributions of activity are inherent and crucial aspects in network electrophysiology (Banerjee and Ellender, 2009; Uhlhaas et al., 2009; Crumiller et al., 2011).

Burst analysis is necessary in analyzing network activity and the network effects of different *in vitro* treatments (Johnstone et al., 2010). Previously, several different burst detection methods, mostly based on experimentally pre-defined parameters such as interspike interval (ISI) and the number of spikes in bursts (Chiappalone et al., 2005; Turnbull et al., 2005; Wagenaar et al., 2006; Pasquale et al., 2010), have been proposed, for example, to study rat cortical or hippocampal neuronal networks. Burst definitions which are more adaptive to the analyzed network have also been proposed (Pasquale et al., 2010; Kapucu et al., 2012). Such adaptability is called for in the analysis of maturing networks, such as human stem cell derived networks (Kapucu et al., 2012).

In spike analysis, spike waveform cut-outs are sorted, and the waveforms in each resulting class, or cluster, can be averaged to obtain the representative spike waveform types (Gibson et al., 2012). Despite its challenges, spike sorting is required for isolating or identifying single

neuronal cell activities in a population firing in an orchestrated manner (Buzsáki, 2004), and different spike sorting algorithms have been utilized in various studies (Santhanam et al., 2006; Sun et al., 2010; Truccolo et al., 2011). Most related to our work, Illes et al. (2014) utilized raster plots of the sorted spikes.

In this paper, a novel joint analysis of sorted spike waveforms and detected bursts is proposed. The joint analysis provides information on the participation of the spike types in bursts for the particular data at hand. In other words, spike type compositions of the bursts, and their changes, e.g., in time or due to external effects, can be assessed using the proposed framework. To our best knowledge, such a joint analysis has not been proposed previously.

A motivation for the development of the joint analysis has been an earlier study on the relationship between single spike features and network bursting in hippocampal pyramidal cells (Harris et al., 2001), which indicated that conditions that cause high firing rates do not necessarily produce high bursting in pyramidal cells. Moreover, the relation between firing rate and bursting may change differently for bursts with different intraburst ISIs (Harris et al., 2001). This may also be the case with our cells, or with any other neuronal network. If this is the case, increase in the activity of a spike type would not guarantee a higher probability of its participation in bursts. Thus, joint analysis would be necessary to assess the burst participations of different spike types.

The joint analysis is illustrated with simulated data containing spikes with different waveforms, organized as individual spikes and bursts, and demonstrated with real MEA data from *in vitro* human neuronal networks undergoing a pharmacological experiment to alter the networks. We show that the proposed framework yields information on the networks and on

the changes therein, which is not obtainable by spike and burst analysis nor by spike sorting alone.

The methods presented in this paper were implemented in Matlab and run in a standard laptop PC. The Matlab code for the proposed joint framework is publicly freely available in the Matlab Central File Exchange and via www.biomeditech.fi.

2. Materials and methods

In this paper we demonstrate our proposed joint analysis together with the conventional methods. The methods are organized in three Sections: 2.1 Cell preparations and the pharmacological experiment; 2.2 MEA measurements; and 2.3 MEA measurement analysis, describing the spike count statistics, spike sorting, burst detection, the proposed joint analysis (Fig. 1) illustrated with simulated data, and mathematical considerations on the proposed joint analysis.

2.1 Cell preparations and the pharmacological experiment

2.1.1 Cell culturing

Human stem cells were used as the starting material for neuronal cultures (Lappalainen et al., 2010). University of Tampere has ethical approval from Pirkanmaa Hospital District to derivate, culture, and differentiate human embryonic stem cells (Skottman, R05116), and the permission from the National Authority for Medicolegal Affairs (1426/32/300/05) to conduct human stem cell research. After differentiation and subsequent plating on MEAs (Heikkilä et al., 2009), the cultures were grown on the MEAs for seven weeks. Each MEA well was considered as one cell culture.

2.1.2. Pharmacological Experiment

The proposed method is demonstrated by analyzing MEA data measured from 12 neuronal cell cultures which were pharmacologically manipulated for different effects on neuronal networks. The pharmacological experiment consisted of the following phases with MEA data acquired at each phase immediately after pharmacological manipulation or wash, and before any manipulations:

i. Baseline
ii. 1st wash with fresh medium, to observe the effects of immediate medium change
iii. CNQX (20 μmol, AMPA/kainate receptor antagonist 6-cyano-7-nitroquinoxaline-2,3-dione, Abcam), to block AMPA/kainate mediated signaling

iv. CNQX (20 µmol, Abcam) + D-AP5 (30 µmol, D(-)-2-amino-5-phosphonopentanoic acid, Abcam) AMPA/kainate and NMDA receptor antagonist, to block glutamatergic signaling

v. 2nd wash with fresh medium

vi. GABA (100 µmol, Sigma), to boost GABAergic signaling

vii. Bicuculline (30 µmol, $GABA_A$ antagonist bicuculline methiobromide, Sigma), to inhibit GABAergic signaling

2.2 MEA measurements

MEA measurements were performed with the MEA wells sealed with semi-permeable membranes (ALA MEA-MEM, ALA Scientific Instruments, Westbury, NY, USA) or custom made PDMS blocks (Kreutzer et al., 2012). The signals from the MEAs were amplified with a preamplifier MEA1060-Inv-BC (Multi Channel Systems MCS GmbH, Reutlingen, Germany, MCS) and analog filtered and amplified with a filter amplifier FA60S-BC (MCS) (bandwidth: 1 Hz - 8 kHz, total gain: 1100). The temperature was controlled with an external heater unit (TC02, MCS) set to +38 °C, and the cultures were allowed to settle for one minute in the preamplifier before each five minute recording. Analog to digital conversion was performed at 20 kHz sampling frequency with MC_Card (MCS) in a PC computer, and the measurement was controlled via MC_Rack software (MCS). The digitized recordings were further processed with MC_Rack to obtain cleaner high frequency spike information using a 50 Hz notch filter to remove mains noise, and a second order Butterworth highpass filter with 200 Hz cutoff frequency to alleviate baseline fluctuations and low frequency local field potential effects. MCS MEA data was imported to Matlab (MathWorks, Inc., Natick, MA, USA) using Neuroshare library (Neuroshare Library, 2003) for offline analysis.

2.3 MEA measurement analysis

At each phase of the pharmacological experiment (see Section 2.1.2), one 300 s recoding was made from each culture (MEA well). The numbers of independent cultures included in the analyses are given in Table S1 along with the inclusion/exclusion criteria for the different analyses.

2.3.1 Spike count statistics

Traditional spike count (the total numbers of spikes in one recording) was calculated for each recording. Only the MEA wells which exhibited sufficient action potential activity were included in burst detection: It was required that at least 50 spikes were detected from an electrode of a MEA well in any 300 s recording of the baseline or at one of the pharmacological experiment phases. The same criterion has been used previously in burst analysis for human embryonic stem cell derived neuronal networks (Kapucu et al., 2012).

To obtain descriptive statistics for the spike counts at the different phases of the experiment, and to compare them with the respective spike counts in the baseline recordings, data from all electrodes of each well was pooled and medians were calculated over the wells. The upper and lower quartiles were calculated along with the differences between the upper and lower quartiles, i.e., the interquartile ranges (IQRs) containing 50% of the data. In the sequel, IQRs are shown in all relevant figures displaying the results. All the spike count statistics calculations were performed in GraphPad Prism 6 (GraphPad Software, Inc., La Jolla, CA, USA).

2.3.2 Spike detection and sorting

Data analysis was performed on data from a single channel and on data pooled from all electrodes. For the single channel analysis, we selected a channel whose firing rate at baseline was the closest to the average firing rate over all channels at the baseline. The average firing rate for the selected channel at the baseline was approximately 1.61 spikes/s, whereas the average firing rate for all baseline recordings per channel was 1.58 spikes/s with the maximum firing rate 14.04 spikes/s.

For the pooled data analysis, spike sorting was performed per well for each phase of the pharmacological experiment. Spike sorting classifies spikes to classes corresponding to the neuronal action potential waveforms. First, spikes were detected by thresholding at five times the median of the baseline noise, and the spike time stamps and waveform cut-outs (spanning 1 ms prior and 2.2 ms after the maximum of the spike) were stored. The obtained spike waveform cut-outs were sorted using the Wave clus algorithm (Quiroga et al., 2004), which gave the average cluster waveforms and the associated lower and upper standard deviation waveforms. In Wave clus, the cluster size was initially set for the baseline according to the number of spikes to be sorted. All the detected spikes were included in the spike count and spike sorting analysis (the total of 172750 spikes). Minimum cluster size for baseline recordings was five spikes for single electrode analysis (the total of 483 spikes were analyzed for the baseline) and 50 spikes for pooled data (the total of 51230 spikes were analyzed for the baseline). However, the cluster sizes were altered for the different phases of the pharmacological experiment, since the activity and spike counts varied between the phases.

After automatic clustering, supervised tuning of the temperature was performed as suggested in the tutorial of Wave clus (Wave_clus, 2004), improving the spike sorting. Still, such spike sorting is less subjective than completely supervised spike sorting. Tuning the temperature was the only supervised correction performed. After unsupervised clustering, the temperature was tuned to observe if more clusters could be formed: If the average spike waveforms of the new clusters due to tuning could be considered as spike types different from those obtained without tuning, the new clusters were retained.

In this work, the effects of overlapping spikes are later discussed based on the analysis results. This matter has been wider addressed, e.g., by Quiroga et al. (2004). Performances of spike sorting algorithms, including Wave clus, have been addressed by Wild et al. (2012), also providing references to methods aimed at solving the spike overlapping problem.

2.3.3. Spike type identification and labeling

To track the occurrence of the spikes types over the pharmacological experiment, it was necessary to identify the representative spike types, and label all the average waveforms observed at the different phases of the experiment with the spike types. This was done by selecting the representative average waveforms as spike types, as described below, and performing correlation analysis of the average waveforms and their respective standard deviation waveforms with those of the spike type waveforms. A simple operator-guided method was devised for the single electrode data analysis and a fully automated method for the full data analysis.

For the single electrode data analysis, the most prominent and distinguished average spike waveforms amongst all the average waveforms for the entire experiment were selected as the representative spike types by visual assessment. Thereafter, cross correlations between each of the remaining average waveforms with all the spike type waveforms were calculated, and the waveforms were tentatively labeled with spike types according to the highest cross correlations. Thus, each cluster produced by Wave clus was assigned a tentative spike label. To take into account the waveform variability, analogous cross correlation analysis was also performed between the standard deviation waveforms: To confirm the tentative spike type labeling, the highest cross correlations had to be found between the standard deviation waveforms of the tentatively labeled cluster and the corresponding standard deviation waveforms of its tentative spike type. Otherwise, the average waveform was considered to represent a new spike type.

For the full data analysis, an automated version of the above cross correlation analysis was devised: Instead of visual identification of the spike types, the average waveforms given by Wave clus for the baseline measurements were used as the spike types. Thereafter, the cross correlation analysis to label the average waveforms with spike types, and the adoption of new spikes types was performed alike described for the single electrode data analysis.

2.3.4 Burst detection

To analyze network activity, an adaptive burst detection algorithm, the cumulative moving average algorithm (CMA) (Kapucu et al., 2012), was employed. CMA utilizes ISI statistics to objectively define and detect bursts. Here, CMA was employed with the same parameters as

in (Kapucu et al., 2012). The exclusion/inclusion criterion was the same as for the spike count statistics (see Table S1).

2.3.5 The proposed joint analysis

In our proposed joint analysis (Fig. 1), first, spikes are detected and sorted. In parallel with spike sorting, burst detection is performed. After spike sorting and burst detection, every detected spike is labeled as either a burst spike or an individual spike, and carries a spike type label. Thus, the participation of different types of spikes in the network activity is unraveled. The wells which did not exhibit any bursting were excluded from the joint analysis of spike types and bursts (see Table S1).

Here, the joint analysis was implemented with the spike detection, spike sorting, and burst detection methods described earlier. To illustrate the proposed joint analysis, we simulated noisy single channel MEA data carrying spikes of three different waveforms (denoted as ASp 1, ASp 2, and ASp 3). The waveforms were modified from the data in the Wave clus distribution package (Wave_clus, 2004). The ISIs were set to at least 30 ms for the spikes in bursts and 300 ms for the individual spikes. Thus, no spike overlapping was introduced to concentrate on the joint analysis without having to consider the performances of spike detection and sorting for overlapping spikes. A 60 s simulation exhibited ten bursts with seven ASp 1s and three ASp 2s in each burst. Four spikes (one ASp 1, one ASp 2 and two ASp 3s) were placed between all bursts. Background noise added to the formed spike signal was a random signal with uniformly distributed values between -3 mV and 3 mV. The spike waveforms are shown in Fig. 2A, and a section of the simulated signal in Fig. 2C. From the

simulated signal, spikes were detected and sorted, and burst and joint analysis were performed to illustrate the methodology.

In the results of this illustrative toy analysis, three average spike waveforms (Fig. 2A), i.e., the spike types, appeared as expected and were sorted with 100% accuracy. The burst detection result (Fig. 2B) shows that all the bursts were correctly detected. An exemplary burst shown in Fig. 2C illustrates the outcome of the proposed analysis framework: **the spike type composition of the burst**. The burst shown in Fig. 2C was composed of the spikes of types ASp 1 and ASp 2 as expected, with one individual ASp3 types spike observed before the burst. The obtained numbers of spikes of different types in bursts and outside of the bursts are presented in Fig. 2D, from which it is seen that all the bursts were composed solely of the spikes of types ASp 1 and ASp 2, whereas spikes of all spike types appeared as individual spikes outside of the bursts, which was 100% in accordance with the simulation setup.

2.3.6 Mathematical considerations regarding the proposed joint analysis

To formulate a mathematical expression of the spike compositions of the bursts in a measurement, a measured signal during a burst with the different identified spike type waveforms can be expressed as

$$s_i(t) = \sum_{j=1}^{J_i} w_{swt_{i,j},t_{i,j}^o}(t) + n_i(t)$$

where $s_i(t)$ is the measured signal sample at discrete time t during the ith burst; J_i is the number of the detected spikes in the ith burst; and $w_{swt_{i,j},t_{i,j}^o}(t)$ is the sample of a spike

waveform signal (of the length of the *i*th burst in samples) which is zero except for the period $t_{i,j}^0 \leq t \leq t_{i,j}^0 + L - 1$ during which the L samples long *swt*th type spike waveform occurs ($swt_{i,j}$ denotes that the type of the *j*th spike of the *i*th burst is *swt*). $n_i(t)$ is the corresponding measured background noise sample accounting for all other signal components except for the identified spike type waveforms. This formulation effectively dissects the bursts in to their constituent spike types. The spike type compositions of the bursts in an entire measured signal is then given by all the pairs $\{swt_{i,j}, t_{i,j}^0\}$.

The information gain due to the proposed joint analysis compared to merely detecting the burst spikes corresponds to that of observing a string of letters formed from the alphabet of the size equal to the number of the spike types plus one (each letter corresponding to a spike type and a symbol '0' to denote 'no waveform') vs. a binary string ('1' corresponding to a detected spike). For example, with three detected spike waveform types denoted A, B, and C, the information gain would result from observing a burst as a string, for example, like '00A0B0000A0CC' (for illustrative purposes, only a few 0s are shown), as compared to observing the same burst with mere spike detection as '0010100001011. Here, possible spike overlapping has not been considered. For the binary alphabet with equal symbol probabilities, the information content is $\log_2(2) = 1$ bit per symbol, whereas an alphabet of size four with equal symbol probabilities results in the information content of $\log_2(4) = 2$ bits per symbol (Shannon, 1948). Naturally the same amount of information per spike waveform is provided by spike sorting alone, but with the proposed joint analysis, this information is extracted specifically for each burst. For a real MEA measurement, the probability of an occurrence of the 'no waveform' symbol is much larger than that of a symbol denoting a spike; thus, the information contents of the spike symbols are larger than in the example, but the principal difference between the two approaches remains. Thereafter, the information gain achievable

by the analyzes of the spike type waveforms themselves, their changes, and their occurrences in time, compared to the analysis of mere time stamps of the burst spikes, depends on the following neurobiological analysis, and the associated information gain is not simply formally quantifiable.

3. Results

To demonstrate the proposed method and the obtainable results, we first present the analysis results for a signal measured via one electrode (Figs. 3 and 4); this example illustrates from phase to phase of the pharmacological experiment, what happened in a vicinity of one electrode, i.e., in a local part of the neuronal network seen via one electrode. Next, we present the analysis results for the entire data set at every phase of the pharmacological experiment. See Table S1 for the number of the cultures at each phase.

3.1 Results of single channel pharmacological experiment data analysis

In the analysis of single electrode data, spike sorting resulted in four different spike types (Fig. 3): one negative and one positive monophasic spike waveform (Spike-I, Fig. 3A, and Spike-II, Fig. 3B), and two biphasic spike waveforms (Spike-III, Fig. 3C, and Spike-IV, Fig. 3D).

Spike counts are shown in Fig. 4A: the total number of spikes detected decreased with the 1st wash compared to the baseline, and also with the application of CNQX. Application of CNQX+D-AP5 increased the number of spikes from that observed with CNQX alone. In the subsequent phases of the pharmacological experiment, the number of spikes did not change

much. On the other hand, observing the numbers of spikes of particular types (Fig. 4B), and the changes in the numbers of spikes of different types relative to the baseline (Fig. 4C), different phenomena can be observed: In the baseline, most of the spikes were of the type Spike-I, which decreased in numbers at the 1st wash and further due to CNQX (Fig. 4B). The number of Spike-II type spikes exhibited a roughly similar trend (Fig. 4B). At the 2nd wash (Fig. 4B) and thereafter, spikes of types Spike-III and Spike-IV were the most prominent. In summary, with the near extinction of spikes of types Spike-I and Spike-II, spikes of types Spike-III and Spike-IV appeared (Fig. 4B). Observing the numbers of spikes of the different types relative to the baseline (Fig. 4C), it is seen that as the pharmacological experiment progressed, the number spike of type Spike-III went through great changes. Since Spike-IV did not appear at baseline, its results cannot be shown relative to the baseline in Fig. 4C. It is clear that the information gained from the analysis of spike statistics for the different spike types (Fig. 4B and C) cannot be obtained from the mere total numbers of spikes (Fig. 4A).

Traditional burst analysis results presented as the relative number of bursts, relative average burst duration, and relative average numbers of spikes in a burst, all compared to their respective baselines, are shown in Fig. 4D-F, respectively. For example: The 1st wash greatly increased the number of bursts, duration, and the number of spikes in a burst (Fig. 4D-F, respectively). CNQX, compared to the previous experiment phase, decreased the relative number of bursts (Fig. 4D), but did not change the burst duration (Fig. 4E), and brought the number of spikes in a burst close to that at the baseline (Fig. 4F). The 2nd wash nearly extinguished bursting activity, whereas the subsequent application of GABA restored approximately half of the number of bursts compared to the baseline (Fig. 4D), and had a tremendous increasing effect on both the burst duration (Fig. 4E) and the number of spikes in a burst (Fig. 4F). Regarding the extreme increase in burst duration for GABA in Fig. 4E, the

average burst duration at the baseline was 0.1 s, whereas after GABA application it was 67.3 s, resulting in the shown 67300% increase in the average duration.

The results of the joint analysis of spike types and bursts are presented in Fig. 4G and H. For clarification, the results in Fig. 4G are presented in Fig. S1A in percentages relative to the total numbers of spikes. To compare the burst spike types and individual spike types for completeness, the different spike types seen in individual spikes are shown in Fig. S2A. To demonstrate the proposed joint analysis, for example, in the baseline the bursts were composed merely of spikes of types Spike-I and II (Fig. 4G), whereas later in the experiment, under CNQX+D-AP5, the bursts were composed far mostly of the spikes of type Spike-II, and the 2nd wash nearly abolished bursting (Fig. 4G and H). However, the picture is totally changed by the application GABA: Under the influence of GABA and thereafter of GABA and bicuculline, the bursts were composed merely of the spikes of types Spike-III and Spike-IV. Thus, the joint analysis of spike types and bursts (Fig. 4G and H) provided more information on the network effects of pharmacological than the traditional burst analysis alone (Fig. 4D-F).

Alike with the spike counts (Fig. 4B and C), also here observing the numbers of spikes in burst (Fig. 4G) and the same relative to the baseline (Fig. 4H), different views to the phenomena are obtained. For example, the increase in the number of Spike-I type spikes after the 1st wash was far greater than that of Spike-II type spikes, but the increase in percentages (Fig. 4H) is roughly equal.

To explicitly point out new information given by the proposed joint analysis, for example, in Fig. 4B it is seen that after the 1st wash, there was a notable decrease in the occurrence of

Spike-I type spikes and a slight decrease in the number of Spike-II type spikes, whereas in Fig. 4D it is seen that simultaneously the number of bursts more than doubled compared to baseline. For this experiment phase, the joint analysis results in Fig. 4G show a notable increase in the burst participation of Spike-I type spikes and slight increase in the burst participation of Spike-II type spikes. This is also reflected in the percentual amounts of the spikes of these types appearing in bursts compared to the total spike counts (Fig. S1A), whereas individual spikes (Fig. S2A) of both types decreased. This information on the changes in the burst participation of the different types of spikes cannot be obtained by the traditional analysis results in Fig. 4B and D.

Also, new information provided by the joint analysis can be demonstrated by observing the activity in Fig. 4B after the CNQX+D-AP5 application when the number of Spike-II type spikes recovered to the approximately same level as it was at the baseline. Spike-I type spikes also recovered approximately to the same level as Spike-II type spikes, however remaining still greatly fewer than at the baseline. At this point of the experiment, the number of bursts, average burst durations, and the average numbers of spikes in bursts were close to what they had been at the baseline (Fig. 4D, E, and F, respectively). The joint analysis results in Fig. 4G show that at this time, the bursts were mostly composed of Spike-II type spikes, whereas at the baseline, the burst spikes had been mainly Spike-I type spikes. In conclusion, although the traditional burst characteristics (Fig. 4D, E, and F) were approximately equal at base line and after the CNQX+D-AP5 application, the joint analysis revealed that the main burst spike type was different between these two experiment phases. This information on the burst composition change cannot be obtained from results of the traditional analyses in Fig. 4B and D, but only with the proposed joint analysis.

3.2 Results of full pharmacological experiment data analysis

In the analysis of the full data set, data from all the MEAs and MEA wells was pooled (see Table S1), and analyzed for each phase of the pharmacological experiment. The average spike waveforms (Fig. 5) obtained from the pooled data exhibited naturally more variation than the spike waveforms obtained from the signal measured via one electrode (Fig. 3). It is to be noted that the variability in the data was quite large, as seen from the IQRs in Fig. 6; therefore we chose not to draw biological conclusions. Nevertheless, the results clearly demonstrate the usability of the proposed joint analysis. In the analysis results in Fig. 6, the quantities shown are the medians over the analyzed wells with the whiskers covering the 50 % IQRs. For burst durations (Fig. 6E) and the number of spikes in a burst (Fig. 6F), shown are the medians of the per-well averages. (See the numbers of analyzed wells in Table S1).

Spike sorting analysis of the pooled data resulted in five different spike types (Spike-I, Spike-II, Spike-III, Spike-IV, and Spike-V, seen in Fig. 5A-E, respectively). In Fig. 5, the average waveforms for each spike type are shown for the phases of the pharmacological experiment at which they were observable.

For this data, two monophasic (one negative (Spike-I, Fig. 5A), and one positive (Spike-II, Fig. 5B)) and two biphasic spike waveforms were obtained (Spike-III, Fig. 5C, and Spike-IV, Fig. 5D), but not all of them were observed at all phases of the pharmacological experiment. Also obtained was Spike-V (Fig. 5E), which appeared only at the 1st wash and under the influence of CNQX+D-AP5. Spike-V was composed of greatly varying individual spike waveforms which could not be clustered together.

In the spike count analysis (Fig. 6A), variability in the total number of spikes was high at the baseline and 1st wash. At the CNQX application, the median of the total number of spikes decreased drastically and remained low compared to the baseline through the rest of the pharmacological experiment. Alike for the single channel data, more information can be obtained by observing the numbers of spikes of different types (Fig. 6B and C). At baseline, Spike-I and II were observed in higher numbers than the other types of spikes. The 1st wash changed the situation drastically, making the Spike-V the most prominent; let us recall that Spike-V was composed of greatly varying spike waveforms which could not be clustered, i.e., the 1st wash greatly disturbed the spike waveforms. Also, Spike-V did not appear at the baseline, and is thus not shown in Fig. 6C and H. CNQX caused some spikes of types Spike-I and II to reappear, whereas CNQX+D-AP5 caused an uprising of Spike-III type spikes (Fig. 6C), which dominated also at the 2nd wash and at the application of bicuculline. GABA nearly shut down spiking (Fig. 6C). Naturally, the spike-type specific phenomena (Fig. 6B and C) cannot be observed from the mere total number of spikes (Fig. 6A).

Traditional burst analysis results presented as the relative number of bursts, relative median of the well-wise average burst durations, and the relative median of the well-wise average number of spikes in a burst, all compared to their respective baselines, are shown in Fig. 6D-F. The relative number of bursts decreased through the pharmacological experiment (Fig. 6D). Burst duration (Fig. 6E) increased slightly at the 1st wash, and more prominently under the influence of CNQX, whereas the 2nd wash decreased the burst duration. GABA caused a large increase in the burst duration (Fig. 6E), to which bicuculline had little effect. Interestingly, the fraction of the total number of spikes appearing in burst remained approximately constant through the experiment (Fig. 6F).

The proposed joint analysis results (Fig. 6G) reveal that at the baseline, the bursts were composed almost completely composed of the spikes of types Spike-I and II, i.e., the monophasic negative (Fig. 5A) and positive (Fig. 5B) spikes, respectively. (For clarification, the results in Fig. 6G are presented in Fig. S1B as the relative numbers of the burst spikes with respect to the total numbers of spikes in percentages. To compare the burst spike types and individual spike types for completeness, the different spike types seen in individual spikes are shown in Fig. S2B.) This means that the networks were operating with the spikes of types Spike-I and II. The 1st wash caused the burst to be composed of almost entirely of Spike-V type spikes (Fig. 6G) which did not represent a well-defined waveform (Fig. 5E). CNQX partially recovered Spike-I and II type spikes also in bursts, whereas CNQX+D-AP5 again removed them from bursts (Fig. 6G and H). The 2nd wash brought the spikes of types Spike-I and II partially back to the bursts, which were now composed of spikes of types Spike-I, II, III, and IV. Under the influence of GABA, there were almost no spikes in bursts (Fig. 6G and H), as there were almost no bursts (Fig. 6D). Nevertheless, the few remaining bursts had approximately the same number of spikes in a burst as at the baseline (Fig. 6F). Bicuculline caused the bursts to be composed mainly of the spikes of types Spike-I and II (Fig. 6G) with a few Spike-III and IV type spikes also present in the bursts (Fig. 6H).

Again, observing the results as counts (Fig. 6B and G) and in percentages (Fig. 6C and H) provided clearly different and complimentary views to the results. Although in this pooled data experiment the spike type change trends (Fig. 6G and H) in the joint analysis in general followed those observed in the traditional analyses (Fig. 6B and C), the proposed joint analysis of spikes and bursts nevertheless provided the actual data on the spike type compositions of the bursts, which was naturally not obtainable by the means of the traditional analyses.

4. Discussion and conclusions

In this paper, we have proposed a novel analysis method for the joint analysis of action potentials and network events observed in local field potential measurements. The main usage of the proposed method is to test a hypothesis that spike types in bursts and spikes in general have different dynamics, e.g., in response to external effects. We have demonstrated that this hypothesis is worth testing, and that the tool developed will provide deeper information on the activity of neuronal networks and their alterations. The essence of the proposed joint analysis was illustrated by a simulation (Fig. 2C), in which a spike type composition of a burst was seen for the first time. The value of the method was demonstrated by analyzing the MEA measurements from a pharmacological experiment with several different chemical applications; the effects of the pharmacological agents were observed with both traditional spike and burst analysis, and with the proposed joint analysis of spikes and bursts, where we demonstrated that the proposed joint analysis reveals information on the network activity which is not obtainable by the traditional analyses, i.e., **the burst participation of the different types of spikes,** and the changes of this by chemical modification of the neuronal activity.

In the analysis of the pooled data, the overall results were calculated in each phase of the pharmacological experiment per well and not per electrode. With this approach, we aimed to study the general behavior of the networks in the different experimental phases. We are confident that regardless of the variability in our data (Heikkilä et al., 2009; Kapucu et al., 2012), the function of the proposed method was described, and the new information

obtainable by the method demonstrated. We observed that indeed there are different dynamics of spike waveform types contributing to the bursts and spikes in general.

To investigate the stability of the signals, especially motivated by the large deviation seen in Spike-V, we took a look at the stability of the spike waveforms during the 300-second measurement after the 1st wash when the Spike-V appeared (Fig. 6B and G). We analyzed each disjoint 100-second section separately. Especially the first and third 100-second sections of the recording had similar clustering results as the complete recording, exhibiting a cluster of highly varying spike waveforms. However, spike waveforms in the second 100-second section were different. This demonstrates that the network function was changing during the recording. In general, one possible disturbing effect may have been the relatively short 1-minute stabilizing period before the measurement after the MEAs were placed in the measurement device. However, due to the described observed behavior during the 100-second sections, we can assume that a longer stabilizing period would not have resulted in more stable networks.

Another issue is the effect of overlapping spikes. Especially for bursting action potentials, spike sorting has been always challenging (Lewicki, 1998; Quiroga et al., 2004; Wild et al., 2012). In our work, especially for the pooled data, spike sorting represents average waveform types obtained from large datasets. Waveform distortions caused by overlapping spikes can be expected to be seen as average and standard deviation waveforms which greatly differ from the general spike average and standard deviation waveforms. Here, highly distorted spikes which could not be assigned to any cluster during spike sorting, accounted for approximately 3.7% of all the analyzed spikes (3.36% for the burst spikes and 0.34% for the individual spikes). Additionally, average and standard deviation waveforms of the

obtained spike types were consistent over the different phases of the experiment for both burst and individual spikes. In conclusion, even though the effects of overlapping could be seen in our analysis, they are not expected to change our results or conclusions.

Using the proposed method, here, we show that the burst spike types and the spikes in general may have different dynamics. By assessing the results both as percentual changes with respect to the baseline activity for each spike type, and as changes in the actual burst spike counts, different views were gained to the changes in the network activity. In the literature, either absolute counts, such as spike and burst counts (Gopal, 2003; Brewer et al., 2009; Hogberg et al., 2011) or changes of percentual values (Gramowski et al., 2000, Ylä-Outinen et al., 2010) are given. Keefer et al. (2001) and Johnstone et al. (2010) provided the results partially in both forms. However, simultaneous analysis of both quantities has not been common practice, and not utilized in drawing comparative conclusions. Here, we demonstrated the usefulness of utilizing both approaches simultaneously in the joint analysis.

The polarity of the measured waveforms has been described to depend on the location of the neuron relative to the electrode (Henze et al., 2000; Gold et al., 2006). Thus, the observed changes in the spike waveforms and the spike type compositions of the bursts may have resulted from chemical induced functional changes in the cells or networks, morphological effects on the cells, different cell compartments contributing to the measurements, or from any combination of these. Nevertheless, we conclude that the observable effects are not random, but consistent manifestations of the changes in the networks. In long-term experiments, cell movement may also affect spike waveforms, which should naturally be evident also in the controls. Here, the experiment was acute, spike sorting was equally successful in all phases of the pharmacological experiment, and the spike type formation and

assignment worked consistently; thus, the observed changes in spike waveforms due to the pharmacological applications did not interfere with spike sorting. It is also to be noted that the number of spikes available for the analysis may also affect the spike sorting results. Here, spike sorting worked consistently.

The pharmacological effects observed in the joint analysis are clear and interesting. Joint analysis results do provide more information on the network changes. Unraveling the actual reasons for, and the consequences of the observed spike type compositions of the bursts, and their changes due to pharmacological and other treatments, call for detailed studies with in-depth neuronal network analysis providing information on the sources of spikes, including information on active neuronal types and cell compartments. This is naturally called for in any spike sorting based analysis.

4.1 Further applicability

Here, the spike sorting by Quiroga et al. (2004) and burst detection by Kapucu et al. (2012) were employed. However, the proposed joint analysis framework (Fig. 1) can be implemented with any spike sorting and burst detection algorithms appropriate for the measurement data at hand. This is important to facilitate both different analysis approaches, and the different characteristics of spikes and bursts in the *in vitro* networks derived from different species and origins; the differences in network behavior have substantial influence on the applicability of different spike sorting and burst detection methods, and also call for more objective and automated methods (Kapucu et al., 2012). For spike sorting, the advantages and drawbacks of supervised and unsupervised algorithms can be argued: An automatic classification can be corrected or optimized by the user with unsupervised

approaches in a final classification step which makes the approach still supervised but less subjective and less time consuming (Martínez and Quiroga, 2013). Certainly it would be preferable to have an accurate and fully unsupervised algorithm, which still remains a largely open question (Martínez and Quiroga, 2013). The only assumptions imposed by the proposed joint analysis framework itself are that there are sortable action potential waveforms and detectable bursts present in the data.

To possibly alleviate the effects of high variability in the data, the single channel analysis used here merely to demonstrate the method, could also be employed in the analysis of the entire MEA by analyzing each channel separately. Thereafter, should the single channel analyzes produce mutually corroborative results, overall conclusions could be drawn. However, combining the single channel analyses results to an overall result would require the development of a separate statistically valid method. Straighter forward, the analysis of single channel data can be employed to reveal the spatial distributions of the different types of spikes composing the bursts. This analysis technique would be promising, e.g., for tracking the spike waveforms and their network participations. Single electrode data analysis naturally considers the local network in the vicinity of the electrode, whereas the analysis pooled data provides a better view to the overall activity and allows statistical analysis, while possibly losing information on particular local network phenomena.

The proposed joint analysis can be performed on all detected spikes, or alternatively, separately on burst spikes and non-burst spikes. In applying the analysis on such different sets of spikes, one needs to consider the possibly different functions of spikes occurring in different circumstances, such as in bursts or individually (Valiante and Carlen, 2014). Here, our main aim was the analysis of bursts, which can be assumed to manifest actual network

activity. Similarly, instead of bursts, spike trains can be analyzed with the proposed method providing the spike types and their changes in the spike trains. Naturally, the same can be done also with individual spikes, i.e., for the spikes not in bursts or trains as demonstrated in Fig. S2. Thus, complementary information on the different processes in the networks can be obtained by the selection of the data to be analyzed. Given spike sorting and burst and/or train detection methods appropriate for the data at hand, the framework is applicable in the analysis of any electrophysiological data, not only in the analysis of in vitro measurements.

4.2 Conclusions

Currently, there is a great call for methods to analyze neuronal network function from *in vitro* MEA recordings in more detail, for example, for research on basic biological questions such as neuronal network development and learning, for the assessment of various culturing methods, and for drug research and neurotoxicology (Coecke and Price, 2007; LeFew et al., 2013). Here, we propose a new joint analysis method that provides the spike type compositions of the bursts. We showed that the spike type compositions of bursts may change subject to environmental effects. Specifically, based on the presented results, pharmacological substances may affect the spike type compositions of the bursts, which is not seen in traditional spike and burst analysis, including spike sorting as traditionally utilized. Thus, with our joint analysis, more detailed information on the network behavior and its changes can be obtained.

Acknowledgments

The work of F. E. Kapucu has been supported by the Finnish Cultural Foundation, Pirkanmaa Regional Fund, by the Human Spare Parts Project funded by the Finnish Funding Agency for Technology and Innovation (Tekes), and by the 3DNeuroN project in the European Union's Seventh Framework Programme, Future and Emerging Technologies, grant agreement n°296590. The works of M. E.-L. Mäkinen, L. Ylä-Outinen, and S. Narkilahti have been supported by the Human Spare Parts Project funded by the Finnish Funding Agency for Technology and Innovation (Tekes). The work of J. M. A. Tanskanen has been supported by the 3DNeuroN project in the European Union's Seventh Framework Programme, Future and Emerging Technologies, grant agreement n°296590.

References

Alloisio S, Nobile M, Novellino A. Multiparametric characterisation of neuronal network activity for in vitro agrochemical neurotoxicity assessment. NeuroToxicology 2015;48:152-65, http://dx.doi.org/10.1016/j.neuro.2015.03.013.

Bal-Price AK, Suñol C, Weiss DG, van Vliet E, Westerink RHS, Costa LG. Application of *in vitro* neurotoxicity testing for regulatory purposes: Symposium III summary and research needs. NeuroToxicology 2008;29(3):520-31, http://dx.doi.org/10.1016/j.neuro.2008.02.008.

Banerjee A, Ellender TJ. Oscillations in the developing cortex: a mechanism for establishing and synchronizing an early network? J Neurosci 2009;29(48):15029-30, http://dx.doi.org/10.1523/JNEUROSCI.4567-09.2009.

Brewer GJ, Boehler MD, Ide AN, Wheeler BC. Chronic electrical stimulation of cultured hippocampal networks increases spontaneous spike rates. J Neurosci Methods 2009; 184(1): 104-9, http://dx.doi.org/10.1016/j.jneumeth.2009.07.031.

Bużańska L, Jurga M, Stachowiak EK, Stachowiak MK, Domańska-Janik K. Neural stem-like cell line derived from a nonhematopoietic population of human umbilical cord blood. Stem Cells Dev 2006;15(3):391-406, http://dx.doi.org/10.1089/scd.2006.15.391.

Bużańska L, Habich A, Jurga M, Sypecka J, Domańska-Janik K. Human cord blood-derived neural stem cell line—possible implementation in studying neurotoxicity. Toxicol in vitro 2005;19(7):991-9, http://dx.doi.org/10.1016/j.tiv.2005.06.036.

Buzsáki G. Large-scale recording of neuronal ensembles. Nat Neurosci 2004;7(5):446-51, http://dx.doi.org/10.1038/nn1233.

Chiappalone M, Novellino A, Vajda I, Vato A, Martinoia S, van Pelt J. Burst detection algorithms for the analysis of spatio-temporal patterns in cortical networks of neurons. Neurocomputing 2005;65-66:653-62, http://dx.doi.org/10.1016/j.neucom.2004.10.094.

Coecke S, Price A. Why *in vitro* neurotoxicity approaches are not formally validated and used for regulatory purposes: The way forward. 2007 [updated 2007 Dec 6; cited 2013 Nov 1], http://www.alttox.org/ttrc/toxicity-tests/neurotoxicity/way-forward/coecke-price/.

Connors BW, Gutnick MJ, Prince DA. Electrophysiological properties of neocortical neurons *in vitro*. J Neurophysiol 1982;48(6):1302-20, http://jn.physiology.org/content/48/6/1302.

Crumiller M, Knight B, Yu Y, Kaplan E. Estimating the amount of information conveyed by a population of neurons. Front Neurosci 2011;5:90, http://dx.doi.org/10.3389/fnins.2011.00090.

Defranchi E, Novellino A, Whelan M, Vogel S, Ramirez T, van Ravenzwaay B, et al. Feasibility assessment of micro-electrode chip assay as a method of detecting neurotoxicity *in vitro*. Front Neuroeng 2011;4:6, http://dx.doi.org/10.3389/fneng.2011.00006.

Egert U, Schlosshauer B, Fennrich S, Nisch W, Fejtl M, Knott T, et al. A novel organotypic long-term culture of the rat hippocampus on substrate-integrated multielectrode arrays. Brain Res Protoc 1998;2(4):229-42, http://dx.doi.org/10.1016/S1385-299X(98)00013-0.

Gibson S, Jack WJ, Markovic D. Spike sorting: The first step in decoding the brain. IEEE Signal Proc Mag 2012;29(1):124-43, http://dx.doi.org/10.1109/MSP.2011.941880.

Gold C, Henze DA, Koch C, Buzsáki G. On the origin of the extracellular action potential waveform: A modeling study. J Neurophysiol 2006;95:3113-3128, http://dx.doi.org/10.1152/jn.00979.2005.

Gopal KV. Neurotoxic effects of mercury on auditory cortex networks growing on microelectrode arrays: A preliminary analysis. Neurotoxicol Teratol 2003;25(1):69-76, http://dx.doi.org/10.1016/S0892-0362(02)00321-5.

Gramowski A, Schiffmann D, Gross GW. Quantification of acute neurotoxic effects of trimethyltin using neuronal networks cultured on microelectrode arrays. NeuroToxicology 2000;21(3):331-42, http://europepmc.org/abstract/MED/10894123.

Gray CM, McCormick DA. Chattering cells: Superficial pyramidal neurons contributing to the generation of synchronous oscillations in the visual cortex. Science 1996;274(5284):109-13, http://dx.doi.org/10.1126/science.274.5284.109.

Gross GW, Rhoades BK. The use of neuronal networks on multielectrode arrays as biosensors. Biosens Bioelectron 1995;10(6-7):553-67, http://dx.doi.org/10.1016/0956-5663(95)96931-N.

Gross GW, Rieske E, Kreutzberg GW, Meyer A. A new fixed-array multi-microelectrode system designed for long-term monitoring of extracellular single unit neuronal activity *in vitro*. Neurosci Lett 1977;6(2-3):101-5, http://dx.doi.org/10.1016/0304-3940(77)90003-9.

Harris KD, Hirase H, Leinekugel X, Henze DA, Buzsáki G. Temporal interaction between single spikes and complex spike bursts in hippocampal pyramidal cells. Neuron 2001;32(1): 141-49, http://dx.doi.org/10.1016/S0896-6273(01)00447-0.

Heikkilä TJ, Ylä-Outinen L, Tanskanen JMA, Lappalainen RS, Skottman H, Suuronen R, et al. Human embryonic stem cell-derived neuronal cells form spontaneously active neuronal networks *in vitro*. Exp Neurol 2009;218(1):109-16, http://dx.doi.org/10.1016/j.expneurol.2009.04.011.

Henze DA, Borhegyi Z, Csicsvari J, Mamiya A, Harris KD, Buzsáki G. Intracellular features predicted by extracellular recordings in the hippocampus *in vivo*. J Neurophysiol 2000;84(1):390-400, http://jn.physiology.org/content/84/1/390.

Hogberg HT, Sobanski T, Novellino A, Whelan M, Weiss DG, Bal-Price AK. Application of micro-electrode arrays (MEAs) as an emerging technology for developmental neurotoxicity: Evaluation of domoic acid-induced effects in primary cultures of rat cortical neurons. NeuroToxicology 2011;32(1):158-68, http://dx.doi.org/10.1016/j.neuro.2010.10.007.

Illes S, Jakab M, Beyer F, Gelfert R, Couillard-Despres S, Schnitzler A, Ritter M, Aigner L. Intrinsically active and pacemaker neurons in pluripotent stem cell-derived neuronal populations. Stem Cell Reports 2014;2(3):323-36, http://dx.doi.org/10.1016/j.stemcr.2014.01.006.

Johnstone AFM, Gross GW, Weiss DG, Schroeder OH-U, Gramowski A, Shafer T. Microelectrode arrays: A physiologically based neurotoxicity testing platform for the 21st century. NeuroToxicology 2010;31(4):331-50, http://dx.doi.org/10.1016/j.neuro.2010.04.001.

Kandel ER, Spencer WA. Electrophysiology of hippocampal neurons. II. After-potentials and repetitive firing. J Neurophysiol 1961;24(3):243-59, http://jn.physiology.org/content/24/3/243.

Kapucu FE, Tanskanen JMA, Mikkonen JE, Ylä-Outinen L, Narkilahti S, Hyttinen JAK. Burst analysis tool for developing neuronal networks exhibiting highly varying action

potential dynamics. Front Comput Neurosci 2012;6:38, http://dx.doi.org/10.3389/fncom.2012.00038.

Keefer EW, Norton SJ, Boyle NAJ, Talesa V, Gross GW. Acute toxicity screening of novel AChE inhibitors using neuronal networks on microelectrode arrays. NeuroToxicology 2001;22(1):3-12, http://dx.doi.org/10.1016/S0161-813X(00)00014-0.

Kreutzer J, Ylä-Outinen L, Kärnä P, Kaarela T, Mikkonen J, Skottman H, et al. Structured PDMS chambers for enhanced human neuronal cell activity on MEA platforms. J Bionic Eng 2012;9(1):1-10, http://dx.doi.org/10.1016/S1672-6529(11)60091-7.

Lappalainen RS, Salomäki M, Ylä-Outinen L, Heikkilä TJ, Hyttinen JAK, Pihlajamäki H, et al. Similarly derived and cultured hESC lines show variation in their developmental potential towards neuronal cells in long-term culture. Regen Med 2010:5(5):749-62, http://dx.doi.org/10.2217/rme.10.58.

LeFew WR, McConnell ER, Crooks JL, Shafer TJ. Evaluation of microelectrode array data using Bayesian modeling as an approach to screening and prioritization for neurotoxicity testing. NeuroToxicology 2013;36:34-41, http://dx.doi.org/10.1016/j.neuro.2013.02.006.

Lewicki MS. A review of methods for spike sorting: The detection and classification of neural action potentials. Network: Computation in Neural Systems 1998;9(4): R53-R78, http://dx.doi.org/10.1088/0954-898X_9_4_001.

Martínez J and Quiroga RQ. Spike Sorting. In: Quiroga RQ, Panzeri S, editors. Principles of Neural Coding. CRC Press; 2013, p. 61-74, http://dx.doi.org/10.1201/b14756-6.

Neuroshare Library. [Sept. 2003, accessed Mar. 2015], http://www.multichannelsystems.com/software/neuroshare-library

Novellino A, Scelfo B, Palosaari T, Price A, Sobanski T, Shafer TJ, et al. Development of micro-electrode array based tests for neurotoxicity: Assessment of interlaboratory reproducibility with neuroactive chemicals. Front Neuroeng 2011;4:4, http://dx.doi.org/10.3389/fneng.2011.00004.

Pasquale V, Martinoia S, Chiappalone M. A self-adapting approach for the detection of bursts and network bursts in neuronal cultures. J Comput Neurosci 2010;29(1-2):219-29, http://dx.doi.org/10.1007/s10827-009-0175-1

Pine J. Recording action potentials from cultured neurons with extracellular microcircuit electrodes. J Neurosci Methods 1980;2(1):19-31, http://dx.doi.org/10.1016/0165-0270(80)90042-4.

Quiroga RQ, Nadasdy Z, Ben-Shaul Y. Unsupervised spike detection and sorting with wavelets and superparamagnetic clustering. Neural Comput 2004;16(8):1661-87, http://dx.doi.org/10.1162/089976604774201631.

Santhanam G, Ryu SI, Yu BM, Afshar A, Shenoy KV. A high-performance brain-computer interface. Nature 2006;442(7099):195-8, http://dx.doi.org/10.1038/nature04968.

Shannon CE. A mathematical theory of communication. Bell Syst Tech J 1948;XXVII(3):379-423, http://dx.doi.org/10.1002/j.1538-7305.1948.tb01338.x.

Sun JJ, Kilb W, Luhmann HJ. Self-organization of repetitive spike patterns in developing neuronal networks *in vitro*. Eur J Neurosci 2010;32(8):1289-99, http://dx.doi.org/10.1111/j.1460-9568.2010.07383.x.

Thomas CA Jr, Springer PA, Loeb GE, Berwald-Netter Y, Okun LM. A miniature microelectrode array to monitor the bioelectric activity of cultured cells. Exp Cell Res 1972;74(1):61-6, http://dx.doi.org/10.1016/0014-4827(72)90481-8.

Truccolo W, Donoghue JA, Hochberg LR, Eskandar EN, Madsen JR, Anderson WS, et al. Single-neuron dynamics in human focal epilepsy. Nat Neurosci 2011;14(5):635-41, http://dx.doi.org/10.1038/nn.2782.

Turnbull L, Dian E, Gross G. The string method of burst identification in neuronal spike trains. J Neurosci Meth 2005;145(1-2), 23-35, http://dx.doi.org/10.1016/j.jneumeth.2004.11.020.

Uchida T, Suzuki S, Hirano Y, Ito D, Nagayama M, Gohara K. Xenon-induced inhibition of synchronized bursts in a rat cortical neuronal network. Neuroscience 2012; 214:149-58, http://dx.doi.org/10.1016/j.neuroscience.2012.03.063.

Uhlhaas PJ, Pipa G, Lima B, Melloni L, Neuenschwander S, Nikolić D, Singer W. Neural synchrony in cortical networks: History, concept and current status. Front Integr Neurosci 2009;3:17, http://dx.doi.org/10.3389/neuro.07.017.2009.

Valiante TA, Carlen PL. Electrophysiological mechanisms of network control: Bursting in the brain - from cells to networks. In: Faingold C, Blumenfeld H, editors. Neuronal Networks in Brain Function, CNS Disorders, and Therapeutics. London, UK: Academic Press; 2014, p. 121-33, http://dx.doi.org/10.1016/B978-0-12-415804-7.00009-5.

Wagenaar DA, Pine J, Potter SM. An extremely rich repertoire of bursting patterns during the development of cortical cultures. BMC Neurosci 2006;7;7:11, http://dx.doi.org/10.1186/1471-2202-7-11.

Wave_clus: Unsupervised spike detection and sorting. 2004, http://www.vis.caltech.edu/~rodri/Wave_clus/Wave_clus_home.htm. Accessed 9 June 2014.

Wild J, Prekopcsak Z, Sieger T, Novak D, Jech R. Performance comparison of extracellular spike sorting algorithms for single-channel recordings. J Neurosci Meth 2012;203(2):369-76, http://dx.doi.org/10.1016/j.jneumeth.2011.10.013.

Ylä-Outinen L, Heikkilä J, Skottman H, Suuronen R, Äänismaa R, Narkilahti S. Human cell-based micro electrode array platform for studying neurotoxicity. Front Neuroeng 2010;3:111, http://dx.doi.org/10.3389/fneng.2010.00111.

Figure 1.

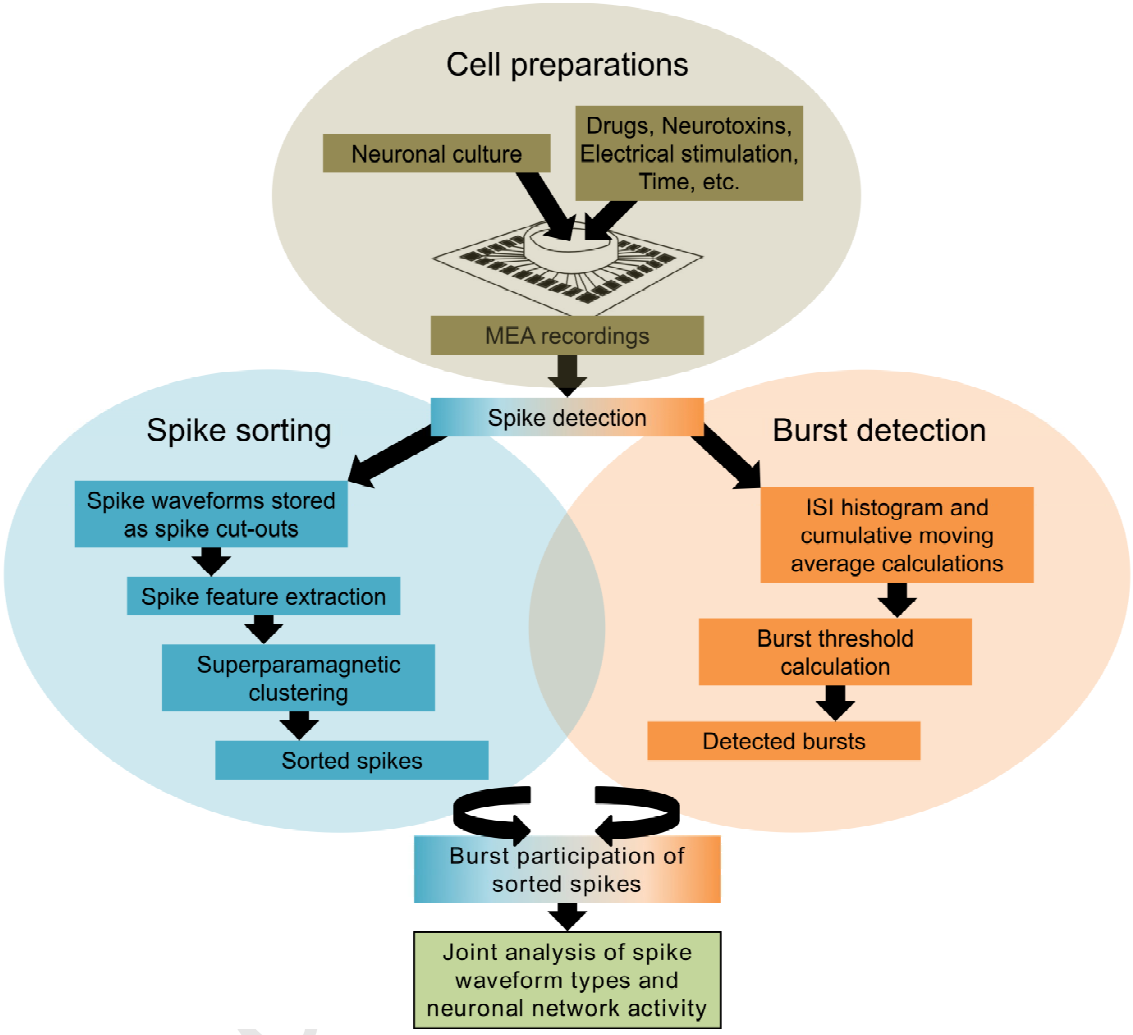

Figure 2

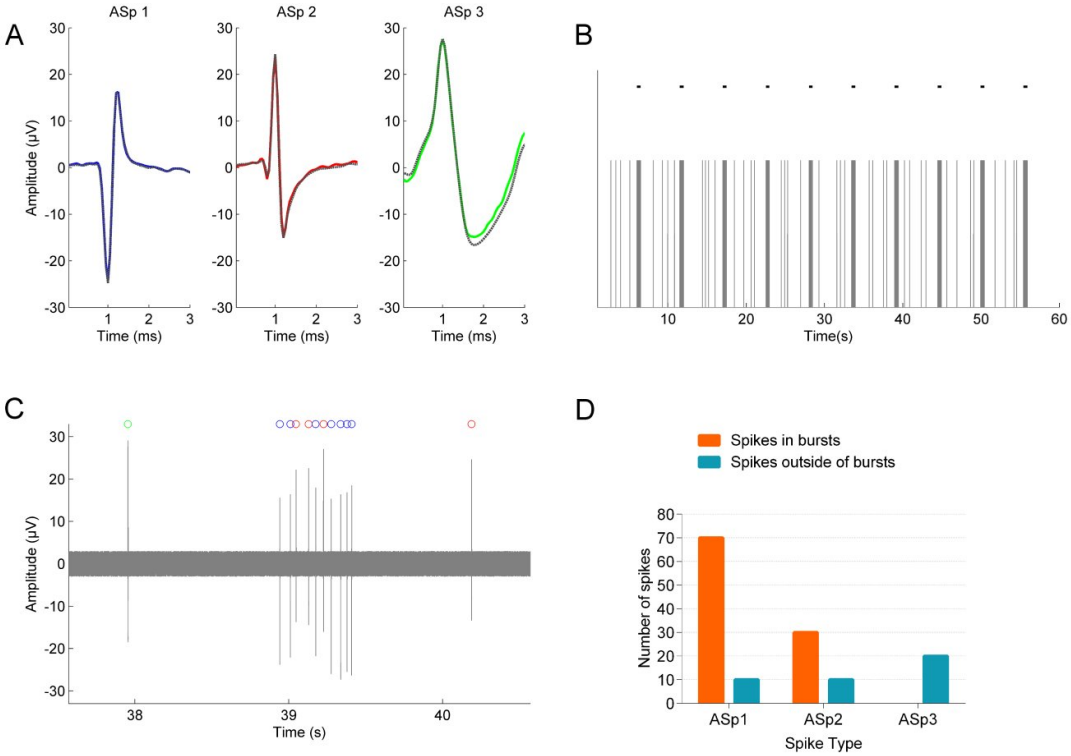

Figure 3

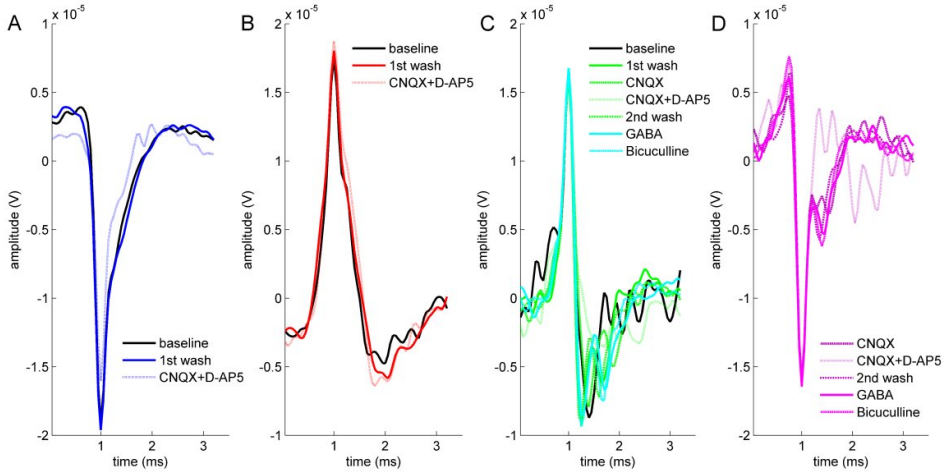

Figure 4

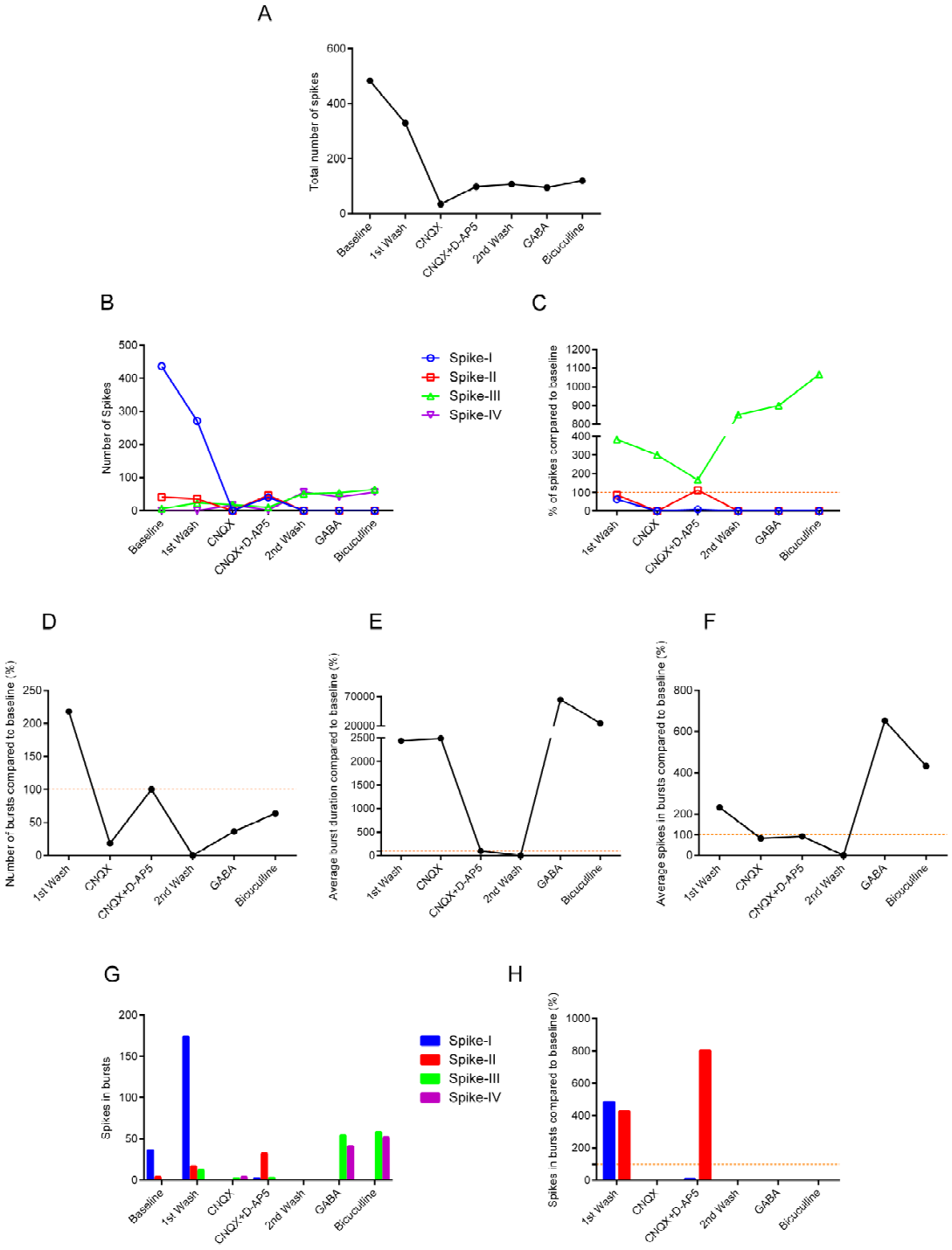

Figure 5

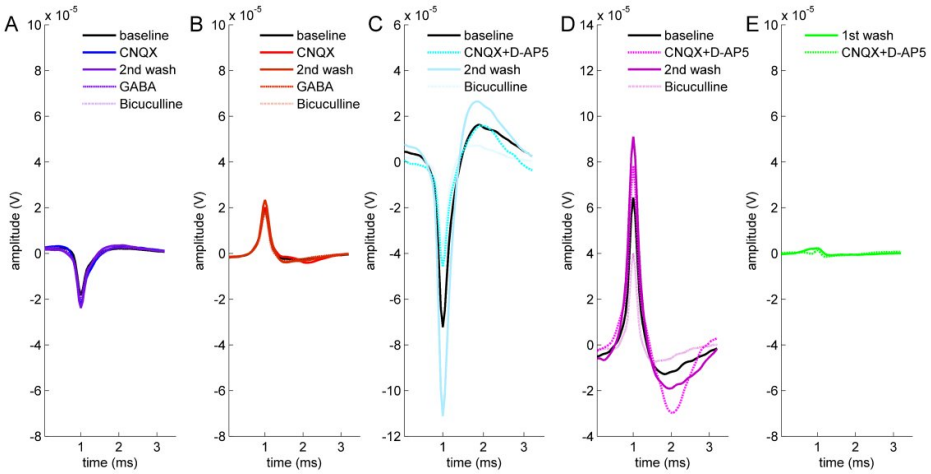

Figure 6

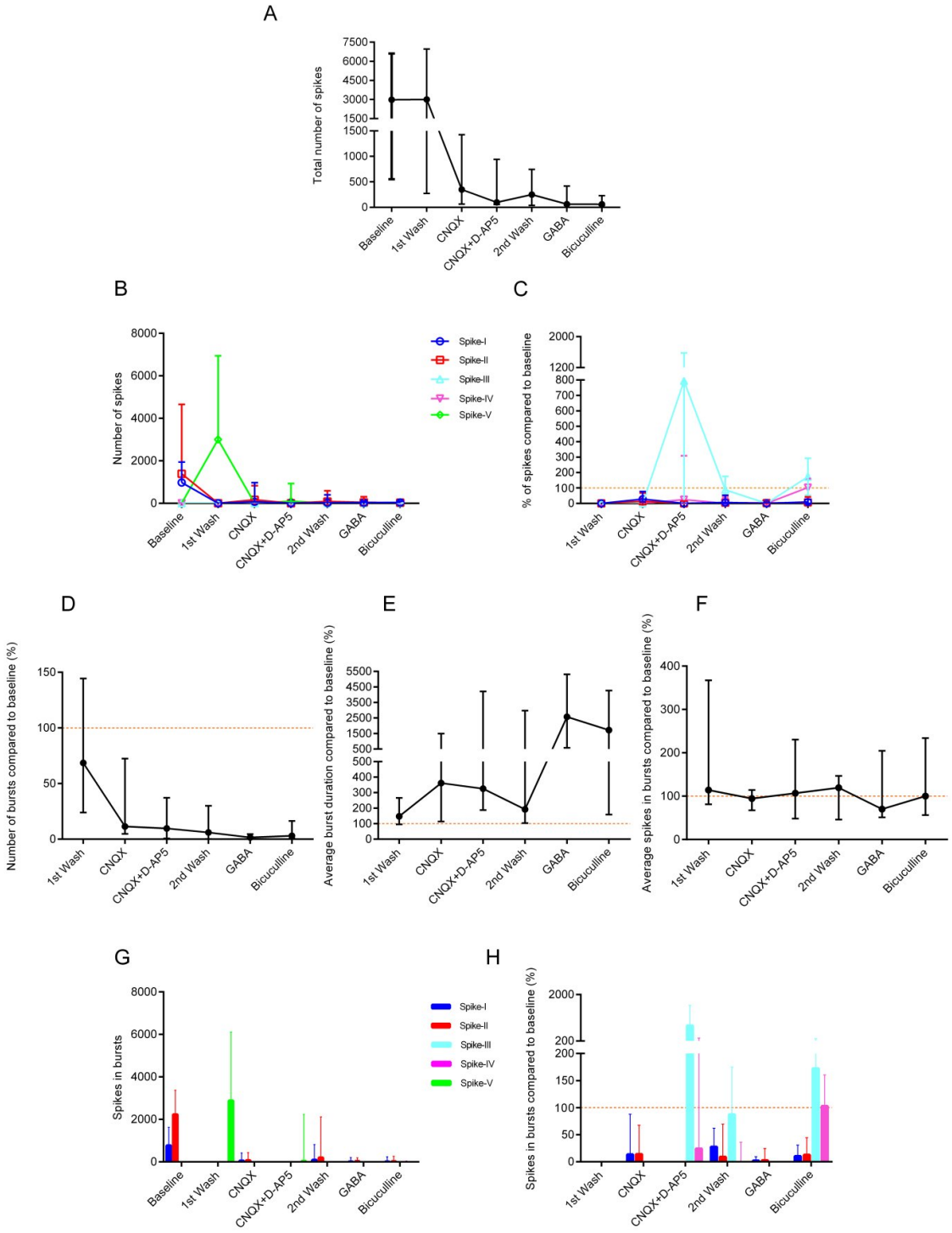

Figure Captions

Fig. 1. A schematic presentation of the proposed joint analysis. The proposed framework consists of spike sorting and burst detection, followed by the analysis of the participation of the spikes of different types observed in bursts. Here, the spike sorting by Quiroga et al. (2004) and burst detection by Kapucu et al. (2012) were employed.

Fig. 2. Simulated toy data and its illustrative joint analysis results. (A) The simulated spike waveforms **ASp 1 (blue)**, **ASp 2 (red)**, and **ASp 3 (green)**, along with the corresponding average waveforms (grey dotted curves) calculated based on the detected and sorted noisy spikes. (B) The time points of the detected spikes (grey vertical bars), and the detected bursts (black horizontal lines). (C) A section of the simulated signal with sorted spikes indicated by circles with the colors indicating the particular waveforms as shown in (A). (D) The results of the joint analysis showing the counts of the different types of spikes participating in the bursts, along with those occurring outside of the bursts.

Fig. 3. The average spike waveforms observed in one channel in the pharmacological experiment, shown for the phases of the pharmacological experiment at which the particular waveforms were observed (see the legend in each panel). The spike types: (A) Spike-I (blue), (B) Spike-II (red), (C) Spike-III (green), and (D) Spike-IV (purple).

Fig. 4. The results of the traditional spike and burst analysis (A-F) and the joint analysis (G and H) at all the phases of the pharmacological experiment for one MEA channel. (A) The total number of spikes. (B) and (C) the numbers of the different types of spikes, and their relative amounts, respectively. (D) The relative numbers of bursts. (E) The relative average durations of bursts. (F) The relative average numbers of spikes in a burst. (G) The numbers of spikes of each type in bursts. (H) The relative numbers of spikes of each type in bursts. The relative quantities are with respect the corresponding values at the respective baselines. The spike types: Spike-I (blue), Spike-II (red), Spike-III (green), and Spike-IV (purple).

Fig. 5. The average spike waveforms observed in the entire pharmacological experiment data set, shown for the phases of the pharmacological experiment at which the particular waveforms were observed (see the legend in each panel). The spike types: (A) Spike-I (blue), (B) Spike-II (red), (C) Spike-III (cyan), (D) Spike-IV (purple), and (C) Spike-V (green).

Fig. 6. The results of the traditional spike and burst analysis (A-F) and the joint analysis (G and H) at all the phases of the pharmacological experiment for the entire data set. (A) The total number of spikes. (B) and (C) the numbers of the different types of spikes, and their relative amounts, respectively. (D) The relative numbers of bursts. (E) The relative average durations of bursts. (F) The relative average numbers of spikes in a burst. (G) The numbers of spikes of each type in bursts. (H) The relative numbers of spikes of each type in bursts. The quantities shown are the medians over the number of analyzed wells (see Table S1) with the whiskers covering the 50 % IQRs. The relative quantities are with respect the corresponding values at the respective baselines. The spike types: Spike-I (blue), Spike-II (red), Spike-III (cyan), Spike-IV (purple), and Spike-V (green).